Contents lists available at ScienceDirect

Journal of Magnetism and Magnetic Materials

journal homepage: www.elsevier.com/locate/jmmm

Orbital structure and magnetic phase diagram of the four-sublattice ferromagnet PbMnBO$_4$

S.N. Martynov

Kirensky Institute of Physics, Federal Research Center, Krasnoyarsk Scientific Center, Siberian Branch, Russian Academy of Sciences, Akademgorodok, Krasnoyarsk, 660036, Russia

ARTICLE INFO

ABSTRACT

A role of quadric and quartic single-ion anisotropy (SIA) of Mn^{3+}-ions, dipole–dipole and Dzyaloshinsky–Moriya (DM) interactions for the magnetic ordering of the four-sublattice ferromagnet PbMnBO$_4$ is investigated. A phase diagram of low-lying magnetic phases on the plane of the DM exchange components is obtained for different values of the SIA parameters. An effect of the isotropic interchain exchange on the spin orientation and, as a result, on the SIA energy in different magnetic phases is considered at the comparable values of the interactions. The determinative role of DM exchange for the magnetic anisotropy of PbMnBO$_4$ is discussed.

1. Introduction

Net crystal magnetic anisotropy is determined by the contributions of several microscopic interactions of the magnetic moments with the crystal lattice and between itself. In noncollinear magnets the moments orientation sufficiently depend on the isotropic exchange interactions between sublattices. So, the orientation of the net magnetization and its dependence on applied magnetic field become a complex function of anisotropic interactions parameters and isotropic exchanges. The determination of the parameters from experimental data is a foreground task at the properties investigation of the concrete magnet.

During a long time the manganese magnets are studied intensively due to variety of magnetic ordering types and multiferroic properties [1,2]. The strong magnetic anisotropy of the crystals with Mn^{3+}-ions (L = 2, S = 2) largely stipulated by the anisotropic character of e_g-functions. The electron occupancy either of the two orbitals ($|3z^2 - r^2\rangle$ or $|x^2 - y^2\rangle$) is accompanied by strong distortion of the ligand octahedral environment. The axes of distorted octahedra are distributed over the crystal lattice with an alternation, that produce orbital ordering. The large orbital and spin moments and spin–orbital interaction lead to strong SIA of Mn^{3+}-ions. At that the principal SIA axes follow the distorted octahedron orientation and locates in the lattice with alternation also. The loss of the symmetry center between magnetic ions surrounded by distorted and rotated octahedron leads to antisymmetric DM exchange. The combined effect of two noncollinearity mechanisms depends on the mutual orientation of the sublattice moments in the states with corresponding magnetic symmetry.

The aim of present work is a determination of the anisotropic interactions effect on the formation of the ground state in the ferromagnetic crystal PbMnBO$_4$.

2. Orbital structure and single-ion anisotropy

PbMnBO$_4$ (space group Pnma) is a rare example of ferromagnetic isolator where a magnetic order is determined by the chains made up of edge-sharing MnO$_6$ octahedra (Fig. 1). The chains are linked by the BO$_3$ and PbO$_4$ groups. The nearest interchain Mn-Mn separation is 5.45 Å while the intrachain one is 2.97 Å. The oxigen octahedra surrounding Mn^{3+}-ions are strongly distorted. The distances between Mn^{3+}-ions and O^{2-}-ions occupying three nonequivalent positions in the octahedron are $s = 1.885$ Å, $m = 1.99$ Å and $l = 2.225$ Å for O$_1$, O$_2$ and O$_3$-ions, respectively [3]. The structure data were achieved by X-ray powder diffraction at room temperature. The parameters of lattice obtained for single crystals in [4] are consistent with the data. The data of X-ray diffraction for $T = 300$ K and 1.5 K [5] shown a minor change of structure in this temperature range. In the present work the structure data are used for calculation of the SIA parameters and explanation of the magnetic measurements [4] in magnetically ordered phase at $T < 31$ K.

The ground electron configuration of manganese ion in a strong crystal field is $t_{2g}^3 e_g^1$. A tetragonal distortion ($l > s, m$) (a static Jahn–Teller effect) split upper electron states $|0\rangle \propto |3z^2 - r^2\rangle/\sqrt{6}$ and $|2^s\rangle = (|2\rangle + |-2\rangle)/\sqrt{2} \propto |x^2 - y^2\rangle/\sqrt{2}$ breaking a degeneracy in a pure octahedral field. Here and after the local z axis is directed along the long Mn–O$_3$ bond. The orthorhombic distortion ($m > s$) entangle the functions. So, yields

$$\Psi_e = \cos\delta|0\rangle - \sin\delta|2^s\rangle,$$
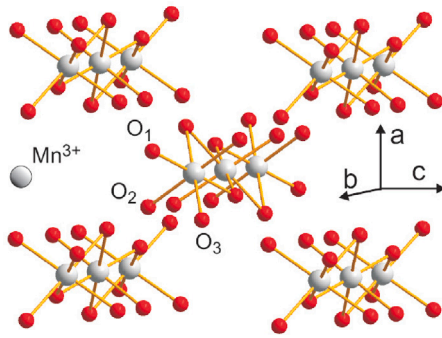$$\Psi_h = \sin\delta|0\rangle + \cos\delta|2^s\rangle, \tag{1}$$

Fig. 1. Chain structure of $PbMnBO_4$. Ions B and Pb are non shown.

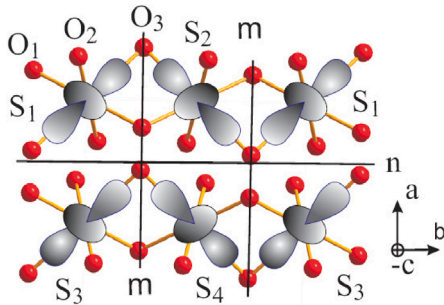**Fig. 2.** The orientation of $Mn^{3+} e_g$-orbitals in the chains with dominant exchange in crystal lattice $PbMnBO_4$. The mirror (m) and diagonal glide (n) planes of symmetry are shown.

- the occupied (electron) and empty (hole) functions [6]. The coefficients of functions are determined by the normal modes of orthorhombic Q_2 and tetragonal Q_3 distortions [7]

$$\tan 2\delta = \frac{Q_2}{Q_3}, \quad Q_2 = \sqrt{2}(m - s),$$

$$Q_3 = \sqrt{\frac{2}{3}}(2l - m - s). \tag{2}$$

Using the crystal data, we obtain $\cos\delta = 0.988$, $\sin\delta = 0.153$. The distribution of the occupied e_g electron function (1) (Fig. 2) corresponds to the electron density distribution calculated in the framework of density functional theory [8].

The quadric SIA energy parameters of Mn^{3+}-ions in tetragonal and orthorhombic crystal field

$$H_{2i} = DS_{zi}^2 + E(S_{xi}^2 - S_{yi}^2), \tag{3}$$

with the axes z_i, x_i and y_i directed along long, middle and short octahedra axes, accordingly, are connected with octahedral distortions (2) [7]

$$\frac{E}{D} = \frac{\tan 2\delta}{\sqrt{3}} = 0.183. \tag{4}$$

For $l > m, s$ the tetragonal component of SIA $D < 0$ defines the local easy axes z_i directed along $O_3 - Mn - O_3$ diagonals in octahedra (Fig. 2). The orthorhombic distortion $m > s$ ($E < 0$) assigns the second easy axes for $O_2 - Mn - O_2$ directions. As a result, all local axes of SIA are distributed over the lattice in the intermediate directions relatively orthorhombic axes.

The quartic single-ion anisotropy affect on the magnetic moments orientation too. In work [9] the orientation of the moments in orbitally ordered antiferromagnet $LaMnO_3$ along the orthorhombic axis was attributed to this anisotropy. For estimation of the effect of this contribution the quartic anisotropy

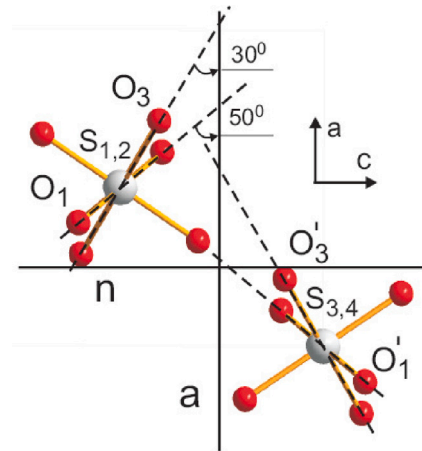$$H_{4i} = a(S_{zi}^4 + S_{xi}^4 + S_{yi}^4) + f S_{zi}^4, \tag{5}$$

Fig. 3. The orientation of O_1 and O_3-planes in the chains $S_1 S_2$ and $S_3 S_4$ with dominant exchange in crystal lattice $PbMnBO_4$. The axial a and diagonal n glide planes of symmetry are shown.

was taken into account with the parameter of the cubic part $a = 0.031 K$ obtained from EPR data for Mn^{3+}-ions in rutile (TiO_2) [10]. Any information about tetragonal quartic parameter f is absent. The anisotropy effect on the energies of magnetic phases was investigated in the range $-a < f < 0$.

3. Crystal structure and two-ion anisotropy

The spatially anisotropic distribution of the manganese ions along the orthorhombic axis **b** (Figs. 1, 2) leads to additional easy-axis dipole–dipole anisotropy along this axis and renormalization of the isotropic exchange

$$H_d = \frac{g^2\mu^2}{b^3}\big(\mathbf{S}_{i,j}\mathbf{S}_{i+1,j} -$$
$$- 3b^{-2}(\mathbf{S}_{i,j}\mathbf{b})(\mathbf{S}_{i,j+1}\mathbf{b})\big) =$$
$$= d \cdot \mathbf{S}_{i,j}\mathbf{S}_{i+1,j} - 3d \cdot S_{i,j}^b S_{i+1,j}^b,$$
$$d = \frac{g^2\mu^2}{b^3}, \tag{6}$$

where b - intrachain distance between neighbors Mn^{3+}-ions. The anisotropic contributions from the next neighbors and interchain interactions are almost canceled and may be neglected. For the dot magnetic dipoles in Mn-chain $3d = 0.28$ K.

The absence of inversion center between magnetic ions results to a requirement of the DM interaction consideration. The inversion center on the magnetic ions defines the distribution of the interaction over the lattice — a staggered DM interaction. At the ground state energy calculations the dominant intrachain exchange allows to limit the consideration of DM exchange between nearest spins in chains only

$$H_{DM} = \mathbf{D}_{12}[\mathbf{S}_1 \times \mathbf{S}_1] + \mathbf{D}_{34}[\mathbf{S}_3 \times \mathbf{S}_4]. \tag{7}$$

The vectors $\mathbf{D}_{12}$ and $\mathbf{D}_{34}$ are located in a mirror plane m (ac) between interacting spins [11] (Fig. 2) and theirs orientations depend on a geometry of exchange bonds. If the exchange is realized over the ligands located in common plane with magnetic ions the DM vector is directed orthogonally to the plane [12–15]. Besides two contributions from separate exchange bonds Mn-O_1–Mn and Mn – O_3 – Mn the two-bridge exchange [16] can exist in $PbMnBO_4$ too (Fig. 2). The direction of the vector of the noncoplanar exchange over two ligands O_1 and O_3 (Fig. 3) unknown initially. This exchange can affect on the value and direction of the vectors $\mathbf{D}_{12}$ and $\mathbf{D}_{34}$ essentially. At the ground state determination it is necessarily take into account two different components of the vectors in the symmetry plane - D_a and D_c.,

directed along the orthorhombic axes **a** and **c**, respectively. Taking into consideration axial (a) and diagonal (n) glide planes between chains (Figs. 2, 3) for the vectors yields $\mathbf{D}_{12}(D_a, 0, D_c)$ and $\mathbf{D}_{34}(-D_a, 0, D_c)$.

4. Phase diagram

In the absence of an external magnetic field, depending on signs and values of the anisotropic interactions, three ground states can exist with the orientation of the total ferromagnetic moment $\mathbf{M} = \mathbf{S}_1 + \mathbf{S}_2 + \mathbf{S}_3 + \mathbf{S}_4$ along each crystal axis with different magnetic symmetries: phase A ($\mathbf{M} \parallel \mathbf{a}$) with symmetry $Pnm'a'$, phase B ($\mathbf{M} \parallel \mathbf{b}$) with symmetry $Pn'ma'$ and phase C ($\mathbf{M} \parallel \mathbf{c}$) with symmetry $Pn'm'a$. The relations between anisotropy parameters, allowing the experimentally observed phase A, are determined by numerical minimization of the energy in the classical spin approximation

$$
\begin{aligned}
E =\ & \frac{N}{2}\Big((J_1 + d)(\mathbf{S}_1\mathbf{S}_2 + \mathbf{S}_3\mathbf{S}_4) + \\
& + 2J_2(\mathbf{S}_1\mathbf{S}_3 + \mathbf{S}_2\mathbf{S}_4) + \\
& + \frac{1}{2}\sum_{i=1}^{4}\big(DS_{zi}^2 + E(S_{xi}^2 - S_{yi}^2) + \\
& + a(S_{zi}^4 + S_{xi}^4 + S_{yi}^4)\big) + \\
& + \mathbf{D}_{12}[\mathbf{S}_1 \times \mathbf{S}_2] + \mathbf{D}_{34}[\mathbf{S}_3 \times \mathbf{S}_4] - \\
& - 3d \cdot (S_1^b S_2^b + S_3^b S_4^b)\Big).
\end{aligned}
\tag{8}
$$

The intra- and interchain exchanges J_1 and J_2 were obtained from the ordering temperature $T_c = 30.3$ K and the paramagnetic Curie temperature $\Theta = 49$ K using the Ginsburg–Landau field theory, describing the quasi-one-dimensional behavior of PbMnBO$_4$: $J_1 + d = -20.2$ K, $J_2 = -2.2$ K [17]. The symmetry constraints reduce the number of independent variables to two angles of spins orientations. For two phases with minimal energies yields

A-phase($Pnm'a'$) : $\mathbf{S}_1(\Theta, \phi)$, $\mathbf{S}_2(\pi - \Theta, \phi)$,

$\mathbf{S}_3(\Theta, -\phi)$, $\mathbf{S}_4(\pi - \Theta, -\phi)$;

B-phase($Pn'ma'$) : $\mathbf{S}_1(\Theta, \phi)$, $\mathbf{S}_2(\Theta, \phi + \pi)$,

$\mathbf{S}_3(\Theta, -\phi)$, $\mathbf{S}_4(\Theta, \pi - \phi)$,

where the polar angles Θ are determined from orthorhombic axis **b** and azimuth one ϕ - from **a**. The energy of magnetic phases (8) was calculated by the standard program of minimization on the orientation angles of the classical spins S_1–S_4 in the Wolfram Mathematica package. Minimizing and comparing the phase energies (8), for the different values of SIA and DM interaction components we obtain the areas of ground states A and B on the plane of normalized values D_a/J_1 and D_c/J_1 (Fig. 4). At the absence of DM interaction ($D_a = D_c = 0$), and quartic anisotropy ($a = 0$) for $|D| < |D_0| = 4.7$ K the ground state is the phase B. A shift of the phase boundaries at the change of tetragonal easy axis anisotropy D is induced by change of spin orientation relatively ab-plane. At low SIA the moments are directed approximately along the axis **a** in phase A and along the axis **b** in phase B. In the case the angles between moments in phase A and easy anisotropy axes z_i $\alpha \approx 50°$ are bigger than the angles in phase B $\alpha \approx 48°$. So, the SIA energy and dipole–dipole anisotropy form the ground state B. An increase of SIA ($D < zJ_2/2 = -4.04$ K) leads to deviation of magnetic moments in the phase A from axis a to the plane of easy axes O_3 (Fig. 3) and the angles between spins and axes z_i are decreased. As a result, the SIA energy in phase A is decreased too. So, without DM interaction the observed phase A can be realized at the strong SIA.

The quartic SIA (5) variously increases the energy of each phase. In the collinear limit ($J_{1,2} \gg D$) the difference between energies of phases A and B

$$
E_4^{A,B} = S^4\Big(a \cdot \sum_{1}^{3}\cos^4\phi_i^{A,B} + f \cdot \cos^4 z_i^{A,B}\Big),
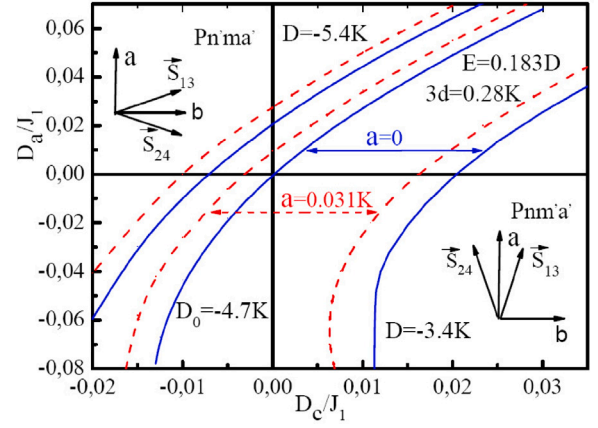$$

Fig. 4. The phase diagram of the ground states A and B on the plane of the DM interaction components for different parameters SIA. The shift of the phase boundaries at $a > 0$ (the dash lines) increases the area of ground state A.
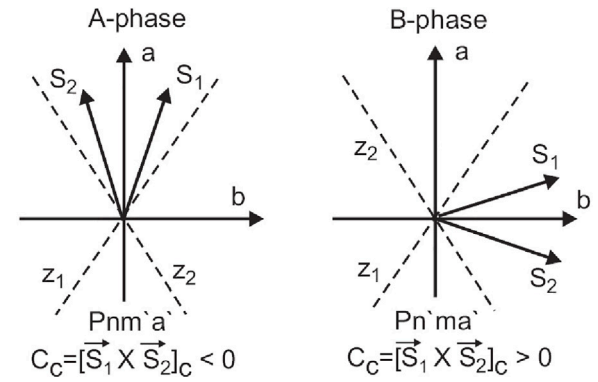

Fig. 5. The different chirality in phases A and B.

where $\phi_i^{A,B}$ - the angles between $\mathbf{S}_i$ and local axes x_i, y_i, z_i in corresponding phases, is equal to ≈ -0.1 K for both f = 0 and f = - a. For considered values of SIA and DM interaction quartic SIA leads to shift of the phase boundaries on an approximately equal step, increasing the area of ground state A (Fig. 4). The phase boundaries at $-a < f < 0$ are situated between corresponding solid and dash lines.

The positive component $D_c > 0$ decreases the energy in phase A and increases one in phase B - the phase A become ground state at the less SIA (Fig. 4).

5. Discussions

The large tetragonal component of SIA $D = -4.9$ K was obtained from EPR investigation of Mn^{3+}-ions in rutile (TiO$_2$) [10]. But even so large SIA is insufficient for explanation of the strong magnetic anisotropy of PbMnBO$_4$ without additional anisotropic mechanisms. In the framework of two-sublattice model [18,19] it was shown, that anisotropic field dependence with specific jump of magnetization in PbMnBO$_4$ [4] can be explained by joint effect from SIA (3) and DM interaction (7). In this case the obtained parameter $D = -3$ K becomes comparable to SIA in detail investigated perovskite LaMnO$_3$ with the similar crystal and local symmetry $D = -3.4$ K, $E/D = 0.134$ [20]. The DM interaction parameter $D_c \approx 3.3$ K, obtained from the comparison of the experimental magnetization curves [4] and the model [19], is close to the SIA one. The similar comparison for the four-sublattice model leads to certain increase of the both values due to rotation of the Mn−O$_3$- planes in the chains on the angles ±30° relatively axis **a** (Fig. 3) and the following additional averaging of SIA. On the phase diagram

(Fig. 4) corresponding PbMnBO$_4$ point ($D_a/J_1 \approx 0$, $D_c/J_1 \approx 0,25$) locates far from phase boundary. As a result, a reorientation of the magnetic moment with the jump in the external field applied along the axis **b** is finished at $H_b \approx 20$ kOe.

The above-made analysis of SIA energy shows that intermediate directions of the local axes lead to frustration of SIA and drastically decrease the contribution of this anisotropy in the net magnetic anisotropy. The contributions of SIA and DM interaction in the ground state energy has different functional form. At the separate consideration the energy of SIA is linear on parameter D while the DM interaction energy is quadratic on the parameter D_c ($E_{DM} \propto D_c^2/J$). As a rule at the comparable values of the parameters $|E_{SIA}| \gg |E_{DM}|$. But in a case when the angles between local SIA easy axes and the directions of magnetic moments orientation in the comparing magnetic phases (A- and B-phases in PbMnBO$_4$) are approximately equal, the mutual orientation of moments become the determinative factor. The chirality parameter

$$\mathbf{C} = [\mathbf{S}_1 \times \mathbf{S}_2], \quad ([\mathbf{S}_3 \times \mathbf{S}_4])$$

depends on the orientation of spins relatively SIA easy axes $\mathbf{z}_i$. In A-phase the parameter C is negative, while in the B-phase is positive (Fig. 5). As a result at $D_c > 0$ the $E_{DM} < 0$ in the A-phase and $E_{DM} > 0$ in B-phase. It determine the ground magnetic state Pnm'a' (A-phase) in PbMnBO$_4$. Note also, that the realized analysis allows to determine the direction of DM vector in crystal relatively local axes of SIA.

6. Conclusions

The orbital ordering of the Jahn–Teller ions Mn^{3+} is accompanied by distribution of the local anisotropy axes in lattice. The easy axes directions take an intermediate positions relatively of lattice axes with an alternation. The experimentally observed ground state with magnetic symmetry Pnm'a' (A-phase) is realized due to DM interaction component pointed along the orthorhombic axis **c**. This component decreases the ground state energy of the A-phase and increases one of the B-phase with symmetry Pn'ma'. The quartic SIA decreases the energy of A-phase relatively B-phase and shifts the boundary between the phases.

Declaration of competing interest

The authors declare that they have no known competing financial interests or personal relationships that could have appeared to influence the work reported in this paper.

Data availability

No data was used for the research described in the article.

Acknowledgment

References

[1] Y. Tokura, N. Nagaosa, Orbital physics in transition metal oxides, Science 288 (2000) 462, http://dx.doi.org/10.1126/science.288.5465.462.

[2] M. Mochizuki, N. Furukawa, Microscopic model and phase diagrams of the multiferroic perovckite manganites, Phys. Rev. B 80 (2000) 134416, http://dx.doi.org/10.1103/PhysRevB.80.134416.

[3] H. Park, R. Lean, J.E. Greedan, J. Barbier, Synthesis, crystal structure, crystal chemistry, and magnetic properties of PbMBO$_4$ (M=Cr,Mn,Fe): a new structure type exhibiting one-dimensional magnetism, Chem. Matter. 15 (2003) 1703, http://dx.doi.org/10.1021/cm0217452CCC.

[4] A. Pankrats, K. Sablina, M. Eremin, A. Balaev, M. Kolkov, V. Tugarinov, A. Bovina, Ferromagnetism and strong magnetic anisotropy of the PbMnBO$_4$ orthoborate single crystals, J. Magn. Magn. Mater. 414 (2016) 82, http://dx.doi.org/10.1016/j.jmmm.2016.04.042.

[5] J. Head, P. Manuel, F. Orlandi, M. Jeong, M. Lees, R. Lee, C. Greaves, Structural, magnetic, magnetocaloric and magnetostrictive properties of Pb$_{1-x}$Sr$_x$MnBO$_4$ (x=0, 0.5, and 1), Chem. Mater. 32 (2020) 10184, http://dx.doi.org/10.1021/acs.chemmater.0c03701.

[6] A. Abragam, B. Bleaney, Electron Paramagnetic Resonance of Transition Ions, Clarendon Press, Oxford, 1970.

[7] J. Kanamori, Crystal distortion in magnetic compound, J. Appl. Phys. 31 (1960) 14S, http://dx.doi.org/10.1063/1.1984590.

[8] H. Xiang, Y. Tang, S. Zhang, Z. He, Intra-chain superexchain couplings in quasi-1D 3d transition metal magnetic compounds, J. Phys.: Condens. Matter 28 (2016) 276003, http://dx.doi.org/10.1088/0953-8984/28/27/276003.

[9] G. Matsumoto, Study of (La$_{1-x}$Ca$_x$)Mn0$_3$. I. Magnetic structure of LaMn0$_3$, J. Phys. Soc. Japan 29 (1970) 606, http://dx.doi.org/10.1143/JPSJ.29.606.

[10] H.J. Gerritsen, E.S. Sabiski, Paramagnetic resonance of trivalent manganeze in rutile TiO$_2$, Phys. Rev. 131 (1963) 1507, http://dx.doi.org/10.1103/PhysRev.131.1507.

[11] T. Moriya, Anisotropic superexchange interaction and weak ferromagnetism, Phys. Rev. 120 (1960) 91, http://dx.doi.org/10.1103/PhysRev.120.91.

[12] F. Keffer, Moriya interaction and the problem of the spin arrangements in MnS, Phys. Rev. 126 (1963) 896, http://dx.doi.org/10.1103/PhysRev.126.896.

[13] A.S. Moskvin, I.G. Bostrem, Some features of the exchange interactions in orthoferrite-orthochromites, Sov. Phys.—Solid State 19 (1977) 1538.

[14] A.S. Moskvin, Microscopic theory of Dzyaloshinsky-Moriya coupling and related exchange-relativistic effects, J. Magn. Magn. Mater. 400 (2016) 117, http://dx.doi.org/10.1116/j.jmmm.2015.07.054.

[15] A.S. Moskvin, Dzyaloshinsky-Moriya antisymmetric exchange coupling in cuprates: oxygen effects, JETP 104 (2007) 913, http://dx.doi.org/10.1134/S106377610706009X.

[16] M.V. Eremin, Y.V. Rakitin, Interference of superexchange interactions, J. Phys. C: Solid State Phys. 15 (1982) L259, http://dx.doi.org/10.1088/0022-3719/15/9/006.

[17] A. Pankrats, M. Kolkov, S. Martynov, S. Popkov, A. Krasikov, M. Gorev, Peculiarities of a magnetic transition in a quasi-one-dimensional ferromagnet PbMnBO$_4$, J. Magn. Magn. Mater. 471 (2019) 416, http://dx.doi.org/10.1016/j.jmmm.2018.09.098.

[18] S.N. Martynov, Single-ion weak antiferromagnetism and spin-flop transition in a two-sublattice ferromagnet, Phys. Solid State 62 (2020) 1165, http://dx.doi.org/10.1134/S1063783420070148.

[19] S.N. Martynov, Ground state of a two-sublattice anisotropic ferromagnet in a magnetic field, Phys. Solid State 63 (2021) 1090, http://dx.doi.org/10.1134/S1063783421080199.

[20] L.E. Gonchar', A.E. Nikiforov, S.E. Popov, Antiferromagnetic resonance spectrum in LaMnO$_3$: interrelation of the orbital structure and the magnetic properties, Sov. Phys.—JETP 91 (2000) 1221, http://dx.doi.org/10.1134/1.1342889.